Modeling and Simulation of a Synchronous Generator Connected to Infinite Bus with an Excitation System in a Bond Graph Approach

GILBERTO GONZALEZ-A[1,3], J. AARON PADILLA GARCIA[3], GERARDO AYALA-JAIMES[2], ARTHUR CLEARY-BALDERAS[3]
[1]Graduate Studies Division, Faculty of Mechanical Engineering,
University of Michoacan,
MEXICO

[2]Faculty of Sciences of Engineering,
Autonomous University of Baja California,
MEXICO

[3]Faculty of Electrical Engineering,
University of Michoacan,
MEXICO

Abstract: The synchronous generator is the essential element is high-power electric energy generation, and its excitation system is vital for understanding its behavior. Thus, a synchronous generator connected to an infinite bus, with its excitation modeled using bond graphs, is proposed. Given the size of these systems which entails certain disadvantages the model is presented in two interconnected stages, with their junction structure defined in a proposed lemma. The mathematical model of the complete system is obtained, and simulation results are shown. Additionally, an external disturbance is applied to the mechanical coupling between the synchronous generator speed and the speed input to the direct current generator, demonstrating that a condition of instability can arise in the excitation and the system as a whole.

Key-Words: - Bond graph, Synchronous generator, Bus infinite, Transmission line.

Received: April 19, 2026. Revised: June 18, 2026. Accepted: August 2, 2026. Published: November 10, 2026.

1 Introduction

The generation and consumption of electrical energy, which is indispensable for all activities today, take place within an electric power energy. Likewise, the fundamental element of an electrical system is the generator, which is synchronous for high power supply capacities.

When modeling synchronous generators, it is common to treat the field winding voltage as a constant source; however, for analyses of stability, generator response, and reactive power behavior, it is essential to consider the generator´s excitation system. References [1, 2, 3] are the best-known and most common in the modeling of the synchronous generator and its excitation system.

Research papers on excitation systems are cited below. Optimal values for the parameters of a synchronous generator, used to determine the mathematical model of the excitation system, are proposed in [4]. The analysis of two modern static excitation systems ST1A and ST7B is developed in [5].The effects of bridge diode switching processes are commonly disregarded, but sometimes this transition can lead to problems in the terminal voltage, which is analyzed in [6]. An excitation with optimal control applied to a synchronous generator is proposed in [7]. The characterization of various types of synchronous generator excitation systems regarding the transient stability of power systems is analyzed in [8]. A simulation of a synchronous generator with mechanical coupling and an excitation system is developed in [9]. Hardware-In-the-Loop technology for examining static excitation systems of synchronous generator is described in [10]. A method for external disturbance rejection control in a synchronous generator excitation system for a ship is proposed in [11]. The stability of multimachine power systems using decentralized excitation control with adaptive sliding modes is improved by [12]. A robust control for the excitation system in the speed stabilization of a synchronous generator is designed in [13]. Excitation control for synchronous generators in multimachine power systems using an adaptive backstepping approach to improve transient stability under parametric uncertainties is presented in [14].

Modeling a synchronous generator with its excitation system represents the coupling of a mechanical subsystem, a three phase AC electrical subsystem, and a DC electrical subsystem; using the bond graph methodology allows these subsystems to be unified within a single reference framework.

Thus, a bond graph is way of graphically representing systems that may consist of multiple energy domains [15]. Furthermore, mathematical models can be derived from a bond graph, and structural properties of the system, such as controllability, observability, decoupling, linearization, steady-state behavior and controller design can be determined [16, 17]. The analysis of structural properties of systems in bond graph can be found in [18, 19].

Likewise, recent advances in bond graph modeling have occurred in various areas, including the behavior of an integrated trigeneration system is simulated and analyzed using bond graph models in [20]. The dynamic bond graph model of a twin rotor system, which is similar to a helicopter, is developed and simulated in [21]. Biomolecular system models are introduced in [22], a bond graph based energy analysis of $Na^+/K^+ - ATPase$ is proposed in [23], a bond graph energy analysis of biochemical oscillators is presented in [24], and the implementation of Julia in systems biology is developed in [25]. Likewise, bond graph model of gear systems are developed in [26, 27].

In this paper, a bond graph model of the system -comprising a synchronous generator, a short transmission line, and an excitation system is proposed. Given the extensive nature of these types of systems, bond graph junction structures for two interconnected subsystems are introduced. In this way, each interconnected bond graph can be modeled independently and analyzed either jointly or separately whether graphically or in terms of its space state mathematical model. To verify the effectiveness of the developed model, simulation results are presented.

Work has been carried out on bond graph modeling of the synchronous generator [28, 29, 30, 31] but without considering the transmission line and the excitation system. The modeling and simulation of a synchronous generator connected to an infinite bus in a bond graph approach is developed in [32]. Another interesting reference related to this paper is the modeling of a balanced system consisting of a synchronous generator and an infinite bus in a multibond graphs approach that is proposed in [33].

Furthermore, to demonstrate the advantages of bond graph system modeling, the behavior of the mechanical coupling speeds, specifically the relationship between the synchronous generator speed and the input speed to the direct current generator is analyzed when the system is subjected to an external disturbance.

Section 2 describes the problem statement regarding the modeling of the generation system including excitation within the traditional differential equation approach. The basic principles of bond graph modeling are defined in Section 3. The synchronous generator connected to the infinite bus - excitation system is proposed in Section 4. The simulation results are presented in Section 5. Finally, the conclusions are given in Section 6.

2 Problem Statement

Consider an electric power generation system connected to the electrical grid via a short transmission line, as shown in Figure 1. The transduction of input mechanical energy (T, w) to three phase electrical energy (a, b, c) is carried out by a synchronous generator (SG), where the transmission line has is characterized by resistance R^l_{abc} and inductance L^l_{abc}, and the electrical grid has a voltage v^{∞}_{abc} [1, 2].

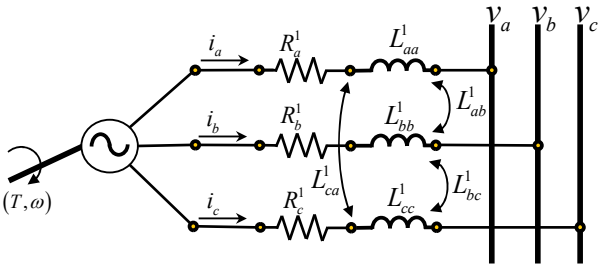


Fig. 1: An electric power system.
Source: created by the authors.

The equations for the electrical system in Figure 1 in (a, b, c) coordinates are defined by

$$v^G_{abc} = R^l_{abc} i_{abc} + L^l_{abc} \frac{di_{abc}}{dt} + v^{\infty}_{abc} \qquad (1)$$

where $v^{\infty}_{abc} = \begin{bmatrix} v^{\infty}_a & v^{\infty}_b & v^{\infty}_c \end{bmatrix}^T$ and $v^G_{abc} = \begin{bmatrix} v^G_a & v^G_b & v^G_c \end{bmatrix}^T$ are the three-phase voltages of the infinite bus and the generator, respectively; R^l_{abc} and L^l_{abc} are the resistance and inductance of the transmission line connecting the generator to the bus and i_{abc} is the generated three-phase current. For a simple transmission line model $R^l_{abc} = diag\left\{R^l_a, R^l_b, R^l_c\right\}$ and $L^l_{abc} = diag\left\{L^l_a, L^l_b, L^l_c\right\}$.

The system of equations given in (1) is a time-varying model; to remove the time dependence, the Park transformation can be applied and is defined by

$$P = \sqrt{\frac{2}{3}} \begin{bmatrix} \cos\theta & \cos\left(\theta - \frac{2\pi}{3}\right) & \cos\left(\theta + \frac{2\pi}{3}\right) \\ \sin\theta & \sin\left(\theta - \frac{2\pi}{3}\right) & \sin\left(\theta + \frac{2\pi}{3}\right) \\ \frac{1}{\sqrt{2}} & \frac{1}{\sqrt{2}} & \frac{1}{\sqrt{2}} \end{bmatrix} \qquad (2)$$

where $\theta = wt + \delta + \frac{\pi}{2}$ being $w = 2\pi F$. This transformation for voltages and currents is given by

$v_{dq0} = Pv_{abc}$ and $i_{dq0} = Pv_{abc}$ then (1) in coordinates $(d, q, 0)$ is transformed to

$$\begin{aligned} Pv^G_{abc} = {} & PR^l_{abc}P^{-1}Pi_{abc} \\ & + PL^l_{abc}P^{-1}P\frac{di_{abc}}{dt} \\ & + Pv^{\infty}_{abc}. \end{aligned} \tag{3}$$

rewriting

$$\begin{aligned} v^G_{dq0} = {} & R^l_{dq0}i_{dq0} + L^l_{dq0}\frac{di_{dq0}}{dt} \\ & - L^l_{dq0}X(w)i_{dq0} + v^{\infty}_{dq0}. \end{aligned} \tag{4}$$

where $R^l_{dq0} = PR^l_{abc}P^{-1}$; $L^l_{dq0} = PL^l_{abc}P^{-1}$ and $X\,(w) = \frac{dP}{dt}P^{-1}$.

Now, the next step to determine the synchronous generator model in $(d, q0)$ coordinates, which is obtained starting from Figure 2 [1, 2].

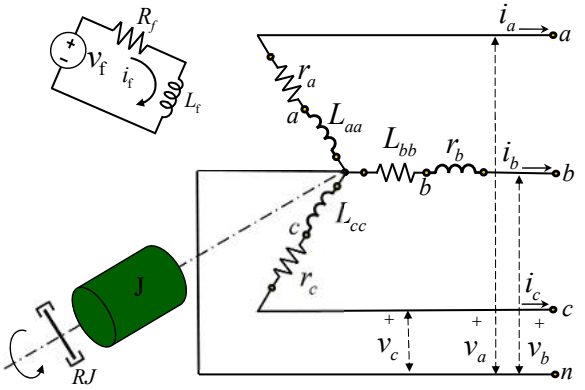


Fig. 2: Synchronous generator in (a, b, c) coordinates.

Source: created by the authors.

The general equation for this generator is

$$\begin{bmatrix} v^G_{abc} \\ v_F \end{bmatrix} = - \begin{bmatrix} R^G_{abc} & 0 \\ 0 & R_F \end{bmatrix} \begin{bmatrix} i_{abc} \\ i_F \end{bmatrix} - \begin{bmatrix} \dot{\lambda}^G_{abc} \\ \dot{\lambda}_F \end{bmatrix}. \tag{5}$$

where v^G_{abc}, i_{abc} and λ^G_{abc} are stator voltages, currents and flux linkages, respectively; v_F, i_F and λ_F are the voltage, current and flux linkage, respectively; and R^G_{abc} and R_F are the resistances of the stator and field winding, respectively.

By applying Park´s transformation to the generator´s stator variables and parameters, the model in $(d, q, 0)$ coordinates is given by

$$\begin{bmatrix} v^G_{dq0} \\ v_F \end{bmatrix} = - \begin{bmatrix} R^G_{dq0} & 0 \\ 0 & R_F \end{bmatrix} \begin{bmatrix} i_{dq0} \\ i_F \end{bmatrix} - \begin{bmatrix} \dot{\lambda}^G_{dq0} \\ \dot{\lambda}_F \end{bmatrix} + \begin{bmatrix} X(w)\lambda_{dq0} \\ 0 \end{bmatrix}. \tag{6}$$

where $R^G_{dq0} = PR^G_{abc}P^{-1} = diag\left\{R^G_d, R^G_q, R^G_0\right\}$.

Flow links are defined by

$$\begin{bmatrix} \lambda^G_{dq0} \\ \lambda_F \end{bmatrix} = \begin{bmatrix} L^G_{dq0} & L_m \\ L^T_m & L_F \end{bmatrix} \begin{bmatrix} i_{dq0} \\ i_F \end{bmatrix} \tag{7}$$

where $L^G_{dq0} = diag\left\{L^G_d, L^G_q, L^G_0\right\}$ and $L^T_m = [\ M_{dF} \quad 0 \quad 0\ ]$.

The generator model is defined by

$$\begin{aligned} \begin{bmatrix} v^G_{dq0} \\ v_F \end{bmatrix} = {} & - \begin{bmatrix} R^G_d & wL^G_q & 0 & 0 \\ -wL^G_d & R^G_q & 0 & -wM_{dF} \\ 0 & 0 & R^G_0 & 0 \\ 0 & 0 & 0 & R_F \end{bmatrix} \begin{bmatrix} i_{dq0} \\ i_F \end{bmatrix} \\ & - \begin{bmatrix} L^G_d & 0 & 0 & M_{dF} \\ 0 & L^G_q & 0 & 0 \\ 0 & 0 & L^G_0 & 0 \\ M_{dF} & 0 & 0 & L_F \end{bmatrix} \frac{d}{dt} \begin{bmatrix} i_{dq0} \\ i_F \end{bmatrix}. \end{aligned} \tag{8}$$

However, it is necessary to take the swing equation into account in order to consider the generator´s mechanical subsystem, which is

$$T_J\frac{dw}{dt} = T_m - Dw \tag{9}$$

where w is the rotor speed, T_m is the input torque to the generator, and D is the friction coefficient.

The following section summarizes the fundamentals of bond graphs.

3 Elements in Bond Graph Modeling

Bond graph is a system modeling methodology that graphically represents the direction of power flow among its elements; through the application of causality, the direction of the generalized power variables is determined, as shown in Figure 3.

The generalized power variables are effort e and flow f, and their characteristic is that their product determines power

$$P = e \bullet f \tag{10}$$

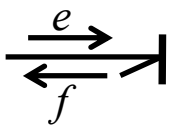


Fig. 3: Causal bond.
Source: created by the authors.

For an electrical system, effort is voltage and flow is current. For the rotational mechanical case, effort is torque and flow is velocity.

The bond graph modeling elements are as follows: The power supply sources designated as (MS_e, MS_f) are active 1-port elements, which are illustrated in Figure 4.

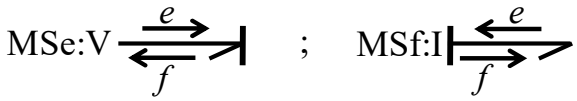


Fig. 4: Power sources.
Source: created by the authors.

The passive elements are defined by the resistors (R), inertias (I) and capacitances (C) shown in Figure 5.

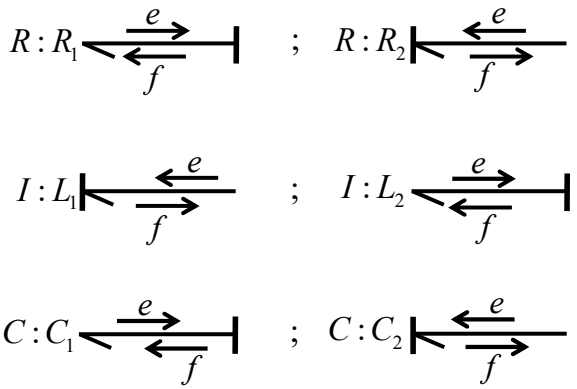


Fig. 5: Passive elements.
Source: created by the authors.

The constitutive relationships of the passive elements are defined by

$$e = R_1 \bullet f;\ f = \frac{1}{R_2} \bullet e \tag{11}$$

$$f = \frac{1}{L_1}\int e dt;\ e = L_2 \frac{df}{dt} \tag{12}$$

$$e = \frac{1}{C_1}\int f dt;\ f = C_2 \frac{de}{dt} \tag{13}$$

There are distributed elements that modulate the variables of a model, known as modulated transformers (MTF) and gyrators (MGY) which are shown in Figure 6.

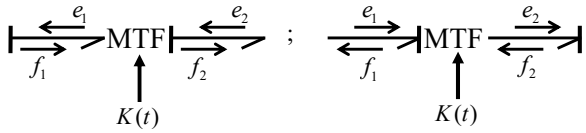


Fig. 6: Transformer and gyrator.
Source: created by the authors.

The connection elements are represented by 0 and 1 junctions shown in Figure 7.

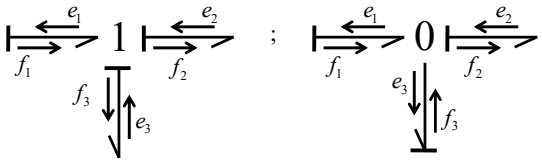


Fig. 7: 0 and 1 junctions.
Source: created by the authors.

According to Figure 7 in a 1-junction it is true that $f_1 = f_2 = f_3$ and $e_1 = e_2 + e_3$ and for 0-junction: $e_1 = e_2 = e_3$ and $f_2 = f_1 + f_3$.

The elements that make up a system can be classified according to how they process power; thus, there are: sources (MS_e, MS_f); energy-storing elements (C, I); dissipative elements (R); sensing elements $(D_e.D_f)$; and junction structure elements $(0, 1, MTF, MGY)$.

Given that a grid connected synchronous generator with an excitation supply is a complex system, this paper proposes a junction structure to subdivide the bond graph modeling of the system, as shown in Figure 8.

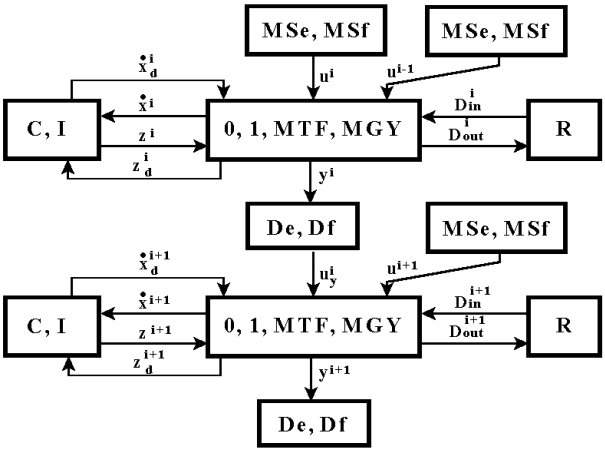


Fig. 8: Subdivided junction structure.
Source: created by the authors.

The junction structure proposed in Figure 8 indicates two subsystems, (i) and $(i+1)$, connected via the output of subsystem (i), and the following lemma determines the mathematical model of a system represented by a bond graph with subsystems.

Lemma

Consider a bond graph modeled system connected via subsystems as shown in Figure 8; the sub-bond graphs are assigned integral causality, and the MTF and MGY elements can be modulated by the co-energy variables z, thereby defining a class of nonlinear systems whose junction structures are defined by

$$\begin{bmatrix} \dot{x}^i \\ D^i_{in} \\ y^i \\ z^i_d \end{bmatrix} = \begin{bmatrix} S^i_{11} & S^i_{12} & S^i_{13} & S^{i-1}_{13} & S^i_{14} \\ S^i_{21} & S^i_{22} & S^i_{23} & S^{i-1}_{23} & 0 \\ S^i_{31} & S^i_{32} & S^i_{33} & S^{i-1}_{33} & 0 \\ S^i_{41} & 0 & S^i_{43} & S^{i-1}_{43} & 0 \end{bmatrix} \begin{bmatrix} z^i \\ D^i_{out} \\ u^i \\ u^{i-1} \\ \dot{x}^i_d \end{bmatrix} \tag{14}$$

$$\begin{bmatrix} \dot{x}^{i+1} \\ D^{i+1}_{in} \\ y^{i+1} \\ z^{i+1}_d \end{bmatrix} = \begin{bmatrix} S^{i+1}_{11} & S^{i+1}_{12} & S^{i+1}_{13} & S^i_{13} & S^{i+1}_{14} \\ S^{i+1}_{21} & S^{i+1}_{22} & S^{i+1}_{23} & S^i_{23} & 0 \\ S^{i+1}_{31} & S^{i+1}_{32} & S^{i+1}_{33} & S^i_{33} & 0 \\ S^{i+1}_{41} & 0 & S^{i+1}_{43} & 0 & 0 \end{bmatrix} \begin{bmatrix} z^{i+1} \\ D^{i+1}_{out} \\ u^{i+1} \\ u^i_y \\ \dot{x}^{i+1}_d \end{bmatrix}. \tag{15}$$

with the constitute relations

$$z^i = F^i x^i \tag{16}$$
$$z^i_d = F^i_d x^i_d \tag{17}$$
$$D^i_{out} = L^i D^i_{in} \tag{18}$$

$$z^{i+1} = F^{i+1} x^{i+1} \tag{19}$$
$$z^{i+1}_d = F^{i+1}_d x^{i+1}_d \tag{20}$$
$$D^{i+1}_{out} = L^{i+1} D^{i+1}_{in} \tag{21}$$

then the state equation in terms of co-energy for stage i is described by

$$\begin{aligned} \dot{z}^i = {} & A^i(z)z^i + B^i(z)u^i \\ & + B^i_{i-1}(z)u^{i-1} + H^i(z)\dot{u}^i \\ & + H^i_{i-1}(z)\dot{u}^{i-1}. \end{aligned} \tag{22}$$

where

$$A^i(z) = \left[E^i\right]^{-1}\left(S^i_{11} + S^i_{12}M^i S^i_{21}\right) \tag{23}$$
$$B^i(z) = \left[E^i\right]^{-1}\left(S^i_{13} + S^i_{12}M^i S^i_{23}\right) \tag{24}$$
$$B^i_{i-1}(z) = \left[E^i\right]^{-1}\left(S^{i-1}_{13} + S^i_{12}M^i S^{i-1}_{23}\right) \tag{25}$$
$$H^i(z) = \left[E^i\right]^{-1} S^i_{14}\left(F^i_d\right)^{-1} S^i_{43} \tag{26}$$
$$H^i_{i-1}(z) = \left[E^i\right]^{-1} S^i_{14}\left(F^i_d\right)^{-1} S^{i-1}_{43} \tag{27}$$
$$E^i = \left(F^i\right)^{-1} - S^i_{14}\left(F^i_d\right)^{-1} S^i_{41} \tag{28}$$

with the output

$$y^i = C^i(z)\,z^i + D^i(z)\,u^i + D^i_{i-1}(z)\,u^{i-1} \tag{29}$$

where

$$C^i(z) = S^i_{31} + S^i_{32}M^i S^i_{21} \tag{30}$$
$$D^i(z) = S^i_{33} + S^i_{32}M^i S^i_{23} \tag{31}$$
$$D^i_{i-1}(z) = S^{i-1}_{33} + S^i_{32}M^i S^{i-1}_{23} \tag{32}$$

with

$$M^i = L^i\left(I - S^i_{22}L^i\right)^{-1} \tag{33}$$

the state equation for stage $i+1$ is given by

$$\begin{aligned} \dot{z}^{i+1} = {} & A^{i+1}(z)z^{i+1} + A^{i+1}_i(z)z^i \\ & + B^{i+1}_{i-1}(z)u^{i-1} + B^{i+1}_i(z)u^i \\ & + B^{i+1}(z)u^{i+1} + H^{i+1}(z)\dot{u}^{i+1} \\ & + H^{i+1}_i(z)\dot{u}^i. \end{aligned} \tag{34}$$

where

$$A^{i+1}(z) = \left[E^{i+1}\right]^{-1} \left(S_{11}^{i+1} + S_{12}^{i+1} M^{i+1} S_{21}^{i+1}\right) \quad (35)$$

$$B^{i+1}(z) = \left[E^{i+1}\right]^{-1} \left(S_{13}^{i+1} + S_{12}^{i+1} M^{i+1} S_{23}^{i+1}\right) \quad (36)$$

$$B_{i+1}^{i}(z) = \left[E^{i+1}\right]^{-1} \left(S_{13}^{i} + S_{12}^{i+1} M^{i+1} S_{23}^{i}\right) \quad (37)$$

$$H^{i+1}(z) = \left[E^{i+1}\right]^{-1} S_{14}^{i+1} \left(F_d^{i+1}\right)^{-1} S_{43}^{i+1} \quad (38)$$

$$H_i^{i+1}(z) = \left[E^{i+1}\right]^{-1} S_{14}^{i+1} \left(F_d^{i+1}\right)^{-1} S_{43}^{i} \quad (39)$$

$$A_i^{i+1}(z) = B^i(z) G^i C^i(z) \quad (40)$$

$$B_{i-1}^{i+1}(z) = B^i(z) G^i D^{i-1}(z) \quad (41)$$

$$B_i^{i+1}(z) = B^i(z) G^i D^i(z) \quad (42)$$

$$E^{i+1} = \left(F^{i+1}\right)^{-1} - S_{14}^{i+1} \left(F_d^{i+1}\right)^{-1} S_{41}^{i+1} \quad (43)$$

with the output

$$y^{i+1} = C^{i+1}(z) z^{i+1} + C_i^{i+1}(z) z^i + D^{i+1}(z) u^{i+1} + D_i^{i+1}(z) u^i + D_{i-1}^{i+1}(z) u^{i-1}. \quad (44)$$

where

$$C^{i+1}(z) = S_{31}^{i+1} + S_{32}^{i+1} M^{i+1} S_{21}^{i+1} \quad (45)$$

$$D^{i+1}(z) = S_{33}^{i+1} + S_{32}^{i+1} M^{i+1} S_{23}^{i+1} \quad (46)$$

$$D_i^{i}(z) = S_{33}^{i+1} + S_{32}^{i+1} M^{i+1} S_{23}^{i+1} \quad (47)$$

and

$$C_i^{i+1}(z) = D_i^i(z) G^i C^i(z) \quad (48)$$

$$D_i^{i+1}(z) = D_i^i(z) G^i D^i(z) \quad (49)$$

$$D_{i-1}^{i+1}(z) = D_i^i(z) G^i D_{i-1}^i(z) \quad (50)$$

with

$$M^{i+1} = L^{i+1} \left(I - S_{22}^{i+1} L^{i+1}\right)^{-1} \quad (51)$$

and the connection between stages i and $i+1$ is given by

$$u_y^i = G^i y^i \quad (52)$$

Proof. Starting from the second line of (14) with (16)

$$D_{in}^i = \left(I - S_{22}^i L^i\right)^{-1} \left(S_{21}^i z^i + S_{23}^i u^i + S_{23}^{i-1} u^{i-1}\right) \quad (53)$$

for the $i+1$ component, from the second line of (15) with (19)

$$D_{in}^{i+1} = \left(I - S_{22}^{i+1} L^{i+1}\right)^{-1} \left(S_{21}^{i+1} z^{i+1} + S_{23}^{i+1} u^{i+1} + S_{23}^i u_y^i\right). \quad (54)$$

the relationship between x^i with x_d^i is obtained from the fourth line (14) with (16) and (17)

$$x_d^i = \left(F_d^i\right)^{-1} S_{41}^i F^i x^i + \left(F_d^i\right)^{-1} S_{43}^i u^i + \left(F_d^i\right)^{-1} S_{43}^{i-1} u^{i-1}. \quad (55)$$

considering that S_{41}^i does not depend on time and differentiating (55)

$$\dot{x}_d^i = \left(F_d^i\right)^{-1} S_{41}^i F^i \dot{x}^i + \left(F_d^i\right)^{-1} S_{43}^i \dot{u}^i + \left(F_d^i\right)^{-1} S_{43}^{i-1} \dot{u}^{i-1}. \quad (56)$$

in a similar way for the $i+1$ component of the fourth line of (15) with (19) and (20)

$$\dot{x}_d^{i+1} = \left(F_d^{i+1}\right)^{-1} S_{41}^{i+1} F^{i+1} \dot{x}^{i+1} + \left(F_d^{i+1}\right)^{-1} S_{43}^{i+1} \dot{u}^{i+1} + \left(F_d^{i+1}\right)^{-1} S_{43}^i \dot{u}^i. \quad (57)$$

Replacing (53) and (56) in the first line of (14) with (33)

$$\begin{aligned} &\left[I - S_{14}^i \left(F_d^i\right)^{-1} S_{41}^i F^i\right] \dot{x}^i \\ &= S_{11}^i z^i \\ &\quad + S_{12}^i M^i \left(S_{21}^i z^i + S_{23}^i u^i + S_{23}^{i-1} u^{i-1}\right) \\ &\quad + S_{13}^{i-1} u^{i-1} + S_{13}^i u^i \\ &\quad + S_{14}^i \left(F_d^i\right)^{-1} S_{43}^i \dot{u}^i \\ &\quad + S_{14}^i \left(F_d^i\right)^{-1} S_{43}^{i-1} \dot{u}^{i-1}. \end{aligned}$$

reducing with (16)

$$\begin{aligned}\dot{z}^i = &\left[\left(F^i\right)^{-1} - S_{14}^i \left(F_d^i\right)^{-1} S_{41}^i\right]^{-1} \\ &\Big[\left(S_{11}^i + S_{12}^i M^i S_{21}^i\right) z^i \\ &+ \left(S_{13}^i + S_{12}^i M^i S_{23}^i\right) u^i \\ &+ \left(S_{13}^{i-1} + S_{12}^i M^i S_{23}^{i-1}\right) u^{i-1} \\ &+ S_{14}^i \left(F_d^i\right)^{-1} S_{43}^i \dot{u}^i \\ &+ S_{14}^i \left(F_d^i\right)^{-1} S_{43}^{i-1} \dot{u}^{i-1}\Big].\end{aligned} \tag{58}$$

by means of equations (28), (23) , (24) , (25) , (26) and (27) combined with (58), state equation (22) is verified.

The output equation for i is obtained from the third line of (14) using (53) and (33)

$$\begin{aligned}y^i = &\left(S_{31}^i + S_{32}^i M^i S_{21}^i\right) z^i \\ &+ \left(S_{33}^i + S_{32}^i M^i S_{23}^i\right) u^i \\ &+ \left(S_{33}^{i-1} + S_{32}^i M^i S_{21}^{i-1}\right) u^{i-1}.\end{aligned} \tag{59}$$

with (30), (31), (32) and (59), the output provided by (29) is verified.

Substituting (54) and (57) in the first line of (15) with (51)

$$\begin{aligned}\dot{x}^{i+1} = &S_{11}^{i+1} z^{i+1} \\ &+ S_{12}^{i+1} M^{i+1} \Big(S_{21}^{i+1} z^{i+1} \\ &\quad + S_{23}^{i+1} u^{i+1} + S_{23}^i u_y^i\Big) \\ &+ S_{13}^{i+1} u^{i+1} + S_{13}^i u_y^i \\ &+ S_{14}^{i+1} \left(F_d^{i+1}\right)^{-1} S_{41}^{i+1} F^{i+1} \dot{x}^{i+1} \\ &+ S_{14}^{i+1} \left(F_d^{i+1}\right)^{-1} S_{43}^{i+1} F^{i+1} \dot{u}^{i+1} \\ &+ S_{14}^{i+1} \left(F_d^{i+1}\right)^{-1} S_{43}^i F^{i+1} \dot{u}^i.\end{aligned} \tag{60}$$

with (19) and (43), expression (60) can be reduced to

$$\begin{aligned}\dot{z}^{i+1} = &\left[E^{i+1}\right]^{-1} \\ &\Big[\left(S_{11}^{i+1} + S_{12}^{i+1} M^{i+1} S_{21}^{i+1}\right) z^{i+1} \\ &+ \left(S_{13}^{i+1} + S_{12}^{i+1} M^{i+1} S_{23}^{i+1}\right) u^{i+1} \\ &+ \left(S_{13}^i + S_{12}^{i+1} M^{i+1} S_{23}^i\right) u_y^i \\ &+ S_{14}^{i+1} \left(F_d^{i+1}\right)^{-1} S_{43}^{i+1} F^{i+1} \dot{u}^{i+1} \\ &+ S_{14}^{i+1} \left(F_d^{i+1}\right)^{-1} S_{43}^i F^{i+1} \dot{u}^i\Big].\end{aligned} \tag{61}$$

based on (61) with (34), expressions (35), (36) , (37) , (38) , (39) and (43) are proven. Thus, (61) can be rewritten as

$$\begin{aligned}\dot{z}^{i+1} = &A^{i+1}(z) z^{i+1} + B^{i+1}(z) u^{i+1} \\ &+ B_{i+1}^i(z) u_y^i \\ &+ H^{i+1}(z) \dot{u}^{i+1} + H_{i-1}^i(z) \dot{u}^{i-1}.\end{aligned} \tag{62}$$

applying (52) to (62) with (29)

$$\begin{aligned}\dot{z}^{i+1} = &A^{i+1}(z) z^{i+1} + B^{i+1}(z) u^{i+1} \\ &+ H^{i+1}(z) \dot{u}^{i+1} + H_{i-1}^i(z) \dot{u}^{i-1} \\ &+ B_{i+1}^i(z) G^i \Big[C^i(z) z^i \\ &\quad + D^i(z) u^i + D_{i-1}^i(z) u^{i-1}\Big].\end{aligned} \tag{63}$$

from (63) with (40), (41) and (42), (34) is verified.

Starting from (54), and the third line of (15) with (33)

$$\begin{aligned}y^{i+1} = &S_{31}^{i+1} z^{i+1} \\ &+ S_{32}^{i+1} M^{i+1} \Big(S_{21}^{i+1} z^{i+1} \\ &\quad + S_{23}^{i+1} u^{i+1} + S_{23}^i u_y^i\Big) \\ &+ S_{33}^{i+1} u^{i+1} + S_{33}^i u_y^i.\end{aligned} \tag{64}$$

with (64), expressions (45), (46) and (47) are proven. The expression (64) with (29) can be written as

$$\begin{aligned}y^{i+1} = &C^{i+1}(z) z^{i+1} + D^{i+1}(z) u^{i+1} \\ &+ D_i^i(z) G^i \Big(C^i(z) z^i \\ &\quad + D_i^i(z) G^i C^i(z) z^i \\ &\quad + D_i^i(z) u^i + D_{i-1}^i(z) u^{i-1}\Big).\end{aligned} \tag{65}$$

by substituting (48), (49) and (50), (44) is proven.

A bond graph model of a generation system is proposed in the next section.

4 Synchronous Generator with Excitation Connected to the Infinite Bus: A Bond Graph Approach

A basic electric power system consisting of a short transmission line connected to a synchronous generator, with a field winding excited by a DC generator is shown in Figure 7.

A bond graph model of a system in Figure 9 is shown in Figure 10. The synchronous generator and the transmission line are in $(d, q, 0)$ coordinates. In Figure 10, the blue dotted line encloses the synchronous generator components, the red dotted line represents the transmission line, the yellow box represents the zero elements coordinate, and the

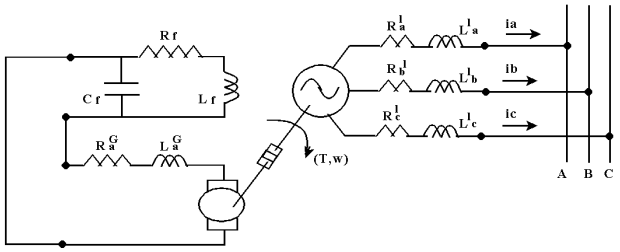


Fig. 9: Synchronous generator with an excitation system.

Source: created by the authors.

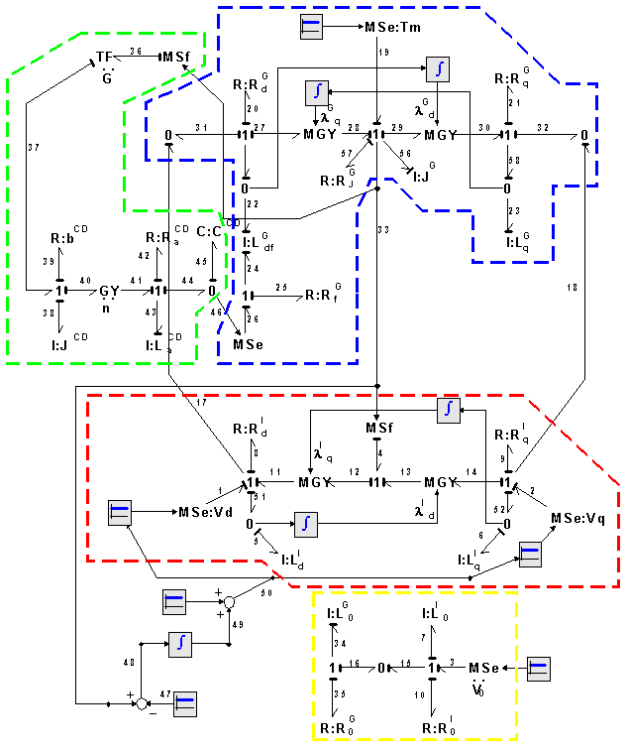


Fig. 10: Bond graph model of the complete system.

Source: created by the authors.

excitation system is contained within the green dotted line.

The main component of an electric power system is the synchronous generator, which in $(d,q,0)$ coordinates, is defined by the resistances R_d^G, R_q^G and R_0^G and the inductances L_{df}^G, L_q^G and L_0^G. The field winding resistance is R_f^G. The input sources are the field winding voltage V_f and the mechanical torque input T_m. The mechanical subsystem contains the inertia of the generator rotor J^G and the friction with the air R_J^G. The mechanical to electrical conversion is performed by gyrators modulated by λ_d^G and λ_q^G.

The transmission line in $(d,q,0)$ coordinates is composed of the resistances $\left(R_d^l, R_q^l, R_0^l\right)$ and inductances $\left(L_d^l, L_q^l, L_0^l\right)$ along each of the axes, respectively. The supply voltages to the system are V_d, V_q and V_0.

The excitation subsystem is defined by a DC generator with inertia J^{CD} and air friction b^{CD}; the armature resistance and inductance R_a^{CD} and L_a^{CD}, respectively. In the generator, mechanical to electrical conversion takes place in GY with a constant module n, and the mechanical connection of the DC generator shaft is established via a transmission factor TF with gain G. A capacitor C^{CD} is connected to the output of the DC generator.

The mathematical model of the system is obtained by applying the proposed lemma. The first stage of the model consists of the synchronous generator connected to the infinite bus, the key vectors of which are as follows:

$$x^i = \begin{bmatrix} p_{22} \\ p_{24} \\ p_{23} \\ p_{56} \\ p_{34} \end{bmatrix}; \overset{\bullet}{x}^i = \begin{bmatrix} e_{22} \\ e_{24} \\ e_{23} \\ e_{56} \\ e_{34} \end{bmatrix}; z^i = \begin{bmatrix} f_{22} \\ f_{24} \\ f_{23} \\ f_{56} \\ f_{34} \end{bmatrix}$$

$$x_d^i = \begin{bmatrix} p_5 \\ p_6 \\ p_7 \end{bmatrix}; \overset{\bullet}{x}_d^i = \begin{bmatrix} e_5 \\ e_6 \\ e_7 \end{bmatrix}; z_d^i = \begin{bmatrix} f_5 \\ f_6 \\ f_7 \end{bmatrix}$$

$$D_{in}^i = \begin{bmatrix} f_{20} & f_{25} & f_{21} & f_{57} & f_{35} & f_8 & f_9 & f_{10} \end{bmatrix}^T$$
$$D_{out}^i = \begin{bmatrix} e_{20} & e_{25} & e_{21} & e_{57} & e_{35} & e_8 & e_9 & e_{10} \end{bmatrix}^T$$
$$u^i = \begin{bmatrix} e_1 & e_2 & e_3 & e_{19} \end{bmatrix}; u^{i-1} = e_{26}; y^i = f_{33}$$

with constitutive relations defined by

$$\left(F^i\right)^{-1} = diag\left\{L_{df}^G, L_q^G, J, L_0^G\right\} \quad (66)$$

$$\left(F_d^i\right)^{-1} = diag\left\{L_d^l, L_q^l, L_0^l\right\} \quad (67)$$

$$L^i = \text{diag}\Big\{R_d^G, R_f^G, R_q^G, R_J, R_0^G, R_d^l, R_q^l, R_0^l\Big\} \quad (68)$$

The i submatrices of the junction structure are given by

$$S_{11}^{i}=\begin{bmatrix} 0 & 0 & 0 & -\lambda_q^G-\lambda_q^l & 0\\ 0 & 0 & 0 & 0 & 0\\ 0 & 0 & 0 & \lambda_d^G+\lambda_d^l & 0\\ \lambda_q^G & 0 & -\lambda_d^G & 0 & 0\\ 0 & 0 & 0 & 0 & 0 \end{bmatrix}$$

$$S_{13}^{i}=\begin{bmatrix} -1 & 0 & 0 & 0\\ 0 & 0 & 0 & 0\\ 0 & -1 & 0 & 0\\ 0 & 0 & 0 & 1\\ 0 & 0 & -1 & 0 \end{bmatrix}, \quad S_{13}^{i-1}=\begin{bmatrix} 0\\ 0\\ 0\\ 1\\ 0 \end{bmatrix}. \tag{69}$$

$$S_{31}^{i}=[0 \quad 0 \quad 0 \quad 1 \quad 0]$$

$$\begin{aligned} S_{14}^{i} &= \begin{bmatrix} 1 & 0 & 0\\ 0 & 0 & 0\\ 0 & 1 & 0\\ 0 & 0 & 0\\ 0 & 0 & 1 \end{bmatrix}; T=\begin{bmatrix} 1 & 0 & 0\\ 0 & 0 & 0\\ 0 & 1 & 0\\ 0 & 0 & 0\\ 0 & 0 & 1 \end{bmatrix}\\ S_{12}^{i} &= [\ -I_5 \quad T\ ] \end{aligned}$$

$$\begin{aligned} S_{21}^{i} &= -\left(S_{12}^{i}\right)^T; S_{41}^{i}=-\left(S_{14}^{i}\right)^T; S_{32}^{i}=S_{33}^{i}=0\\ S_{22}^{i} &= S_{23}^{i}=S_{23}^{i-1}=0 \end{aligned}$$

The key vectors of the $i+1$ subsystem are

$$\begin{aligned} x^{i+1} &= \begin{bmatrix} p_{43}\\ q_{45} \end{bmatrix}; \overset{\bullet}{x}^{i+1}=\begin{bmatrix} e_{43}\\ f_{45} \end{bmatrix}; z^{i+1}=\begin{bmatrix} f_{43}\\ e_{45} \end{bmatrix}\\ x_d^{i+1} &= p_{38}; \overset{\bullet}{x}_d^{i+1}=e_{38}; z_d^{i+1}=f_{38}; u_y^i=f_{36}\\ D_{in}^{i+1} &= \begin{bmatrix} f_{39}\\ f_{42} \end{bmatrix}; D_{out}^{i+1}=\begin{bmatrix} e_{39}\\ e_{42} \end{bmatrix} \end{aligned}$$

with the constitutive relations

$$\left(F_d^{i+1}\right)^{-1} = diag\left\{L_d^l, L_q^l, L_0^l\right\} \tag{70}$$

$$L^{i+1} = diag\left\{J^{CD}, R_a^{CD}\right\} \tag{71}$$

and the junction structure is described by

$$\begin{bmatrix} e_{43}\\ f_{45}\\ f_{39}\\ f_{42}\\ e_{45}\\ f_{38} \end{bmatrix} = \begin{bmatrix} 0 & -1 & 0 & -1 & nG & 0\\ 1 & 0 & 0 & 0 & 0 & 0\\ 0 & 0 & 0 & 0 & G & 0\\ 1 & 0 & 0 & 0 & 0 & 0\\ 0 & 1 & 0 & 0 & 0 & 0\\ 0 & 0 & 0 & 0 & G & 0 \end{bmatrix} \begin{bmatrix} f_{43}\\ e_{45}\\ e_{39}\\ e_{42}\\ f_{36}\\ e_{38} \end{bmatrix}. \tag{72}$$

Applying the lemma, the mathematical model for stage i is described by

$$E^i \overset{\bullet}{z}^i = A^i(z)\, z^i + B^i(z)\, u^i + B_{i-1}^i(z)\, u^{i-1} \tag{73}$$

where

$$E^i=\begin{bmatrix} L_d^G+L_d^l & M & 0 & 0 & 0\\ M & L_f^G & 0 & 0 & 0\\ 0 & 0 & L_q^G+L_q^l & 0 & 0\\ 0 & 0 & 0 & J^G & 0\\ 0 & 0 & 0 & 0 & L_0^G+L_0^l \end{bmatrix} \tag{74}$$

$$E^i A^i(z) = -\begin{bmatrix} R_d^T & 0 & 0 & \lambda_q^G+\lambda_q^l & 0\\ 0 & R_f^G & 0 & 0 & 0\\ 0 & 0 & R_q^T & -\lambda_d^G-\lambda_d^l & 0\\ -\lambda_q^G & 0 & \lambda_d^G & R_J^G & 0\\ 0 & 0 & 0 & 0 & R_0^T \end{bmatrix} \tag{75}$$

$$E^i B^i(z) = \begin{bmatrix} -1 & 0 & 0 & 0\\ 0 & 0 & 0 & 0\\ 0 & -1 & 0 & 0\\ 0 & 0 & 0 & 1\\ 0 & 0 & -1 & 0 \end{bmatrix} \tag{76}$$

$$E^i B_{i-1}^i(z) = [\ 0 \quad 1 \quad 0 \quad 0 \quad 0\ ]^T \tag{77}$$

$$H_i(z) = H_{i-1}^i(z) = 0 \tag{78}$$

where $R_d^T = R_d^G + R_d^l$; $R_q^T = R_q^G + R_q^l$; $R_0^T = R_0^G + R_0^l$.

For stage $i+1$

$$\begin{bmatrix} C^{CD} & 0\\ 0 & L_a^{CD} \end{bmatrix} \begin{bmatrix} \dot{f}_{43}\\ \dot{e}_{45} \end{bmatrix} = \begin{bmatrix} -b^{CD} & -1\\ 1 & 0 \end{bmatrix} \begin{bmatrix} f_{43}\\ e_{45} \end{bmatrix} + \begin{bmatrix} nG\\ 0 \end{bmatrix} u^{i+1} \tag{79}$$

The behavior of the generation system is analyzed through simulations.

5 Simulation Results

The numerical parameters of the system for determining its behavior are as follows: $v_a = 220\sin(wt)\ V$, $v_b = 220\sin(wt - 2\pi/3)\ V$, $v_c = 220\sin(wt + 2\pi/3)$; $T_m = 300\ N \cdot m$; $R_d^G = 0.5\Omega$, $R_q^G = 0.5\Omega$, $R_0^G = 0.5\Omega$, $R_d^l = 2.5\Omega$, $R_q^l = 2.5\Omega$, $R_0^l = 2.5\Omega$, $R_f^G = 0.95\Omega$, $R_J^G = 1\Omega$, $R_d^G = 0.5\Omega$, $R_a^{CD} = 0.01\Omega$, $R_b^{CD} = 1.5\Omega$, $L_q^G = 1.64H$, $L_d^l = 0.001H$, $L_q^l = 0.001H$, $L_0^l = 0.001H$, $L_a^{CD} = 0.01H$, $C^{CD} = 0.9F$, $J^G = 2.37N \cdot m \cdot s^2$, $J^{CD} = 1.4N \cdot m \cdot s^2$ and $L_{df}^G = \begin{bmatrix} 1.7 & 1.55 \\ 1.55 & 1.65 \end{bmatrix}$.

With the given parameters, the behavior of the state variables in terms of co-energy for stage i, that is $z^i = [\ f_{22}\quad f_{24}\quad f_{23}\quad f_{56}\quad f_{34}\ ]^T$ where $f_{22} = i_d^G$, $f_{24} = i_f^G$; $f_{23} = i_Q^G$; $f_{56} = w$ and $f_{34} = i_0^G$ representing the synchronous generator variables are shown in Figure 11.

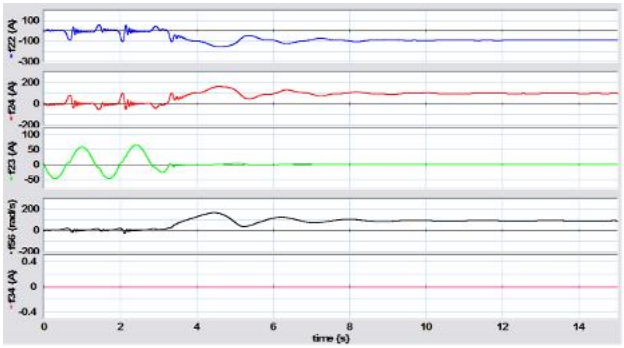


Fig. 11: Response of the variables z^i.
Source: created by the authors.

The steady state values of z^i denoted by $(z^i)_{ss}$ are given by

$$(z^i)_{ss} = \begin{bmatrix} (f_{22})_{ss} \\ (f_{24})_{ss} \\ (f_{23})_{ss} \\ (f_{56})_{ss} \\ (f_{34})_{ss} \end{bmatrix} = \begin{bmatrix} 88.9665A \\ 100.6741A \\ 1.3571A \\ 95.6081rad/s \\ 0A \end{bmatrix} \quad (80)$$

The behavior of the co-energy variables of stage $i+1$, that is $z^{i+1} = [\ f_{43}\quad e_{45}\ ]^T$, where $f_{43} = i_a^{CD}$ and $e_{45} = V_C^{CD}$,the significance of the excitation system variables is shown in Figure 12.

The steady state values of z^{i+1} denoted by $(z^{i+1})_{ss}$ are given by

$$(z^{i+1})_{ss} = \begin{bmatrix} (f_{43})_{ss} \\ (e_{45})_{ss} \end{bmatrix} = \begin{bmatrix} -0.9251A \\ 95.6430V \end{bmatrix} \quad (81)$$

Note that the synchronous generator variables will only begin to stabilize once the excitation system

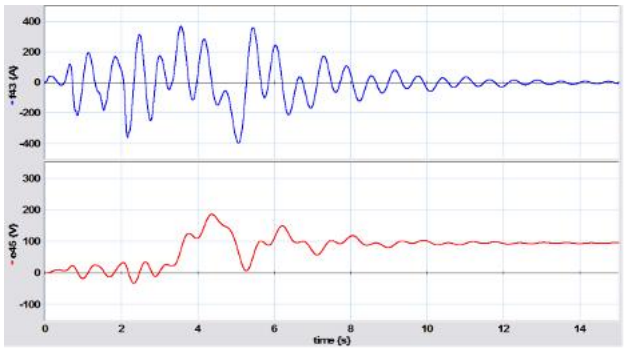


Fig. 12: Response of the variables z^{i+1}.
Source: created by the authors.

voltage has settled at its steady-state value. The system currents (i_a, i_b, i_c) generated and sent from the generator to the transmission line, reaching the infinite bus, are shown in Figure 13 and Figure 14.

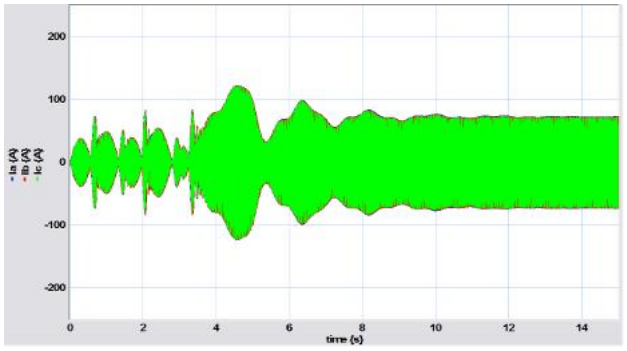


Fig. 13: Response of the generated currents.
Source: created by the authors.

Figure 13 illustrates the full simulation range, while a reduced time interval is shown in Figure 14.

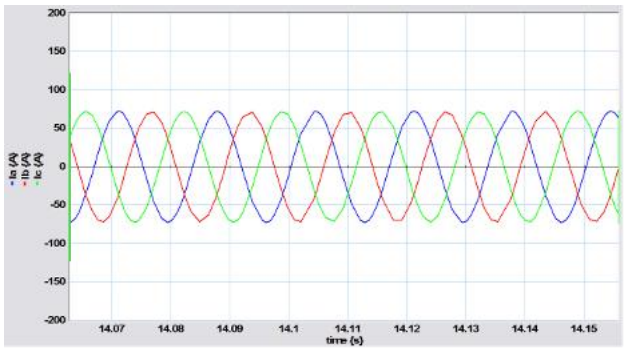


Fig. 14: Response of the currents over a short interval.
Source: created by the authors.

Power is supplied to the generator´s excitation system via a mechanical coupling, providing the DC

generator with the mechanical energy that will be converted into direct current electrical energy. This mechanical coupling in the bond graph is a TF element with bonds 36 and 37; the velocities or flow variables on both bonds, with a constant modulus of 0.1, are shown in Figure 15.

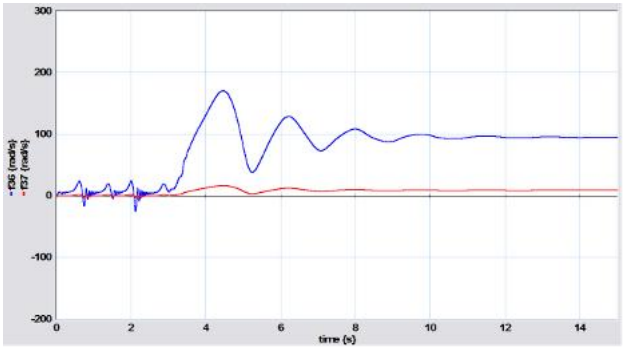


Fig. 15: Mechanical coupling speeds with $G = 0.1$.

Source: created by the authors.

Note that the synchronous generator speed is $w^G = 95.8314 rad/s$ and the input speed to the DC generator is $w^{CD} = 9.5831 rad/s$; after the transient period, the system stabilizes, resulting in a stable power supply from the excitation system to the synchronous generator.

Subsequently, the mechanical coupling is subjected to an external disturbance initiated at $15s$ and ending at $18s$ generated by a cycloidal signal with a maximum magnitude of $G^{ext} = 0.1075$, while the original ratio of $G = 0.1$, Figure 16 shows the behavior of the speeds within the coupling.

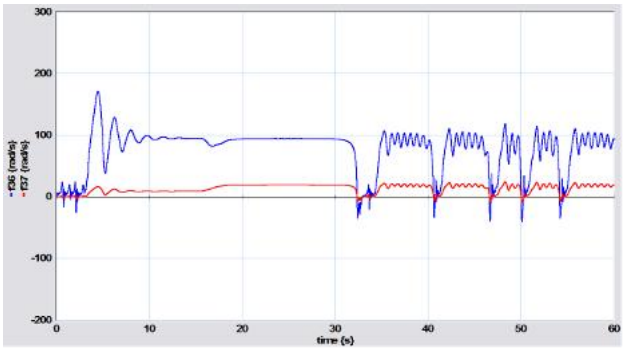


Fig. 16: Coupling speeds with $G^{ext} = 0.1075$.

Source: created by the authors.

The behavior of the currents $(i_d,\ i_f, i_q)$ under this instability condition of $G^{ext} = 0.1075$ is illustrated in Figure 17.

It is clearly evident that, although the external disturbance ended at $18s$ and is increasing $G^T = G + G^{ext} = 0.2$, the velocities were altered in a way that

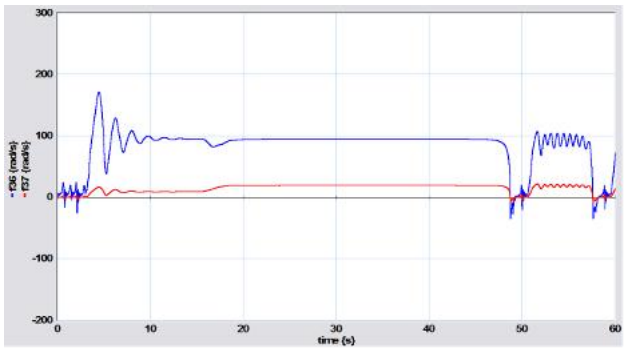


Fig. 17: Currents i_d, i_f and i_q with $G^{ext} = 0.1075$.

Source: created by the authors.

generated an unstable condition throughout the entire system. The disturbance decreased to $G^{ext} = 0.107$ and the system maintains a condition of instability,as shown in Figure 18.

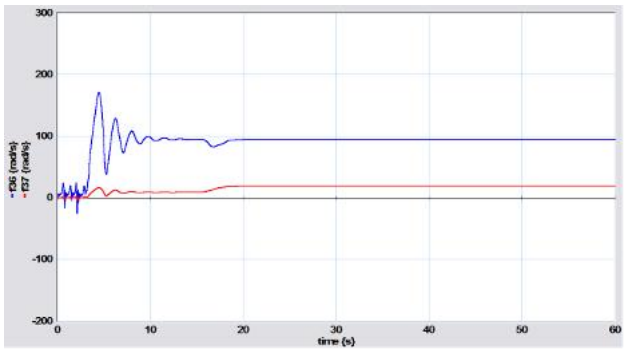


Fig. 18: Coupling speeds with $G^{ext} = 0.107$.

Source: created by the authors.

The performance of the i_d, i_f and i_q currents is shown in Figure 19, where it can be seen the stability is maintained from $20s$ onwards, but the system becomes unstable shortly before $50s$.

It is interesting to note that, with this perturbation, instability appears at $50s$, even though stability seemed to be maintained. By applying the perturbation at $G^{ext} = 0.1$, the system returns to the stable condition, as illustrated in Figure 20.

The behavior of the currents i_d, i_f and i_q is illustrated in Figure 21 which shows that the system is stable.

Through this system stability analysis applying external perturbations of varying magnitudes to the mechanical coupling it is determined that this element is highly sensitive and critical to the stability of the entire system, for if excitation stability is lost, the synchronous generator will also become unstable, and the current supplied to the infinite bus via the transmission line will become unstable potentially, in an extreme case, destabilizing other components

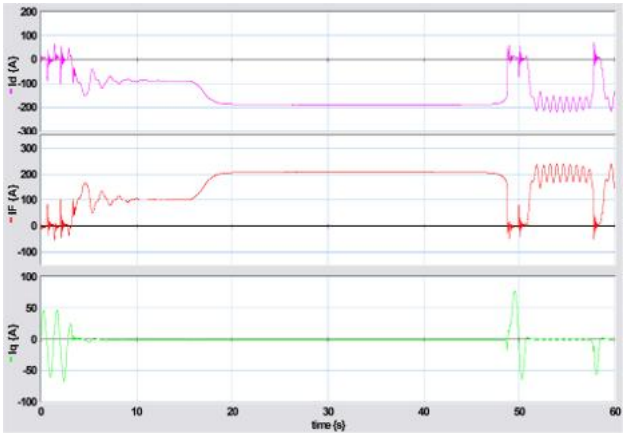


Fig. 19: Currents i_d, i_f and i_q with $G^{ext} = 0.107$.
Source: created by the authors.

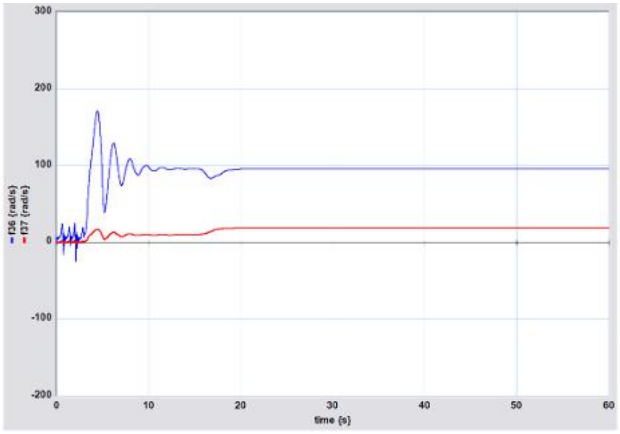


Fig. 20: Coupling speeds with $G^{ext} = 0.1$.
Source: created by the authors.

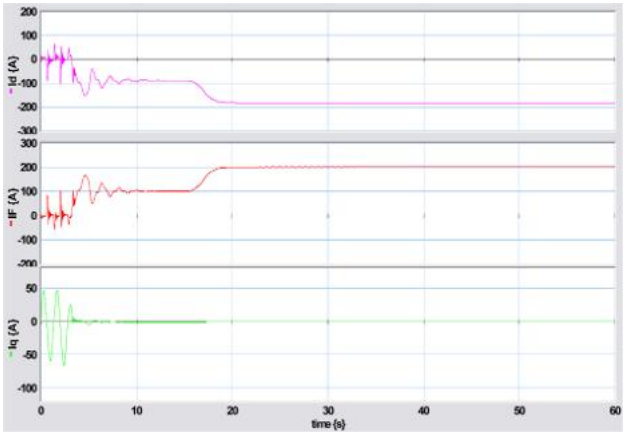


Fig. 21: Currents i_d, i_f and i_q with $G^{ext} = 0.1$.
Source: created by the authors.

connected to that infinite bus.

This paper does not extend to determining the value of the mechanical coupling between the speeds of the synchronous generator and the direct current generator required to maintain system stability. This could be a subject for future work on maintaining stability across a range of values for this coupling.

6 Conclusions

A synchronous generator connected to an infinite bus via a short transmission line, with an excitation system modeled using bond graphs, has been presented. Given that such systems consist of interconnected subsystems, a lemma is proposed to establish junction structures for subsystems in bond graphs. In this way, the mathematical models of the subsystems are obtained. The simulation results using the 20-Sim software are shown. The mechanical coupling between the synchronous generator and the direct current generator is subject to external disturbances, which can lead to instability in the excitation system and the system as a whole.

Declaration of Generative AI and AI-assisted Technologies in the Writing Process

During the preparation of this work, the author(s) utilized artificial intelligence (AI) technologies solely for the purpose of linguistic refinement and grammatical correction. Following the application of these tools, the author(s) comprehensively reviewed, verified, and edited the resulting text. The author(s) maintain full accountability and responsibility for the accuracy, integrity, and final content of the publication.

References:

[1] P. Kundur, *Power System Stability and Control*. New York, NY, USA: McGraw-Hill, 1994.

[2] P. M. Anderson and A. A. Fouad, *Power System Control and Stability*. Ames, IA, USA: The Iowa State University Press, 1977.

[3] P. C. Krause, O. Wasynczuk, and S. D. Sudhoff, *Analysis of Electric Machinery and Drive Systems*, 2nd ed. Piscataway, NJ, USA: IEEE Press, 2002.

[4] Y. A. Ahmed, Y. I. M. Al-Mashhadany, and M. A. Nayyef, "High performance of excitation system for synchronous generator based on modeling analysis," *Bulletin of Electrical Engineering and Informatics*, vol. 9, no. 6, pp. 2235–2243, Dec. 2020, doi: 10.11591/eei.v9i6.2627.

[5] R. B. Binnar and V. P. Mohale, "Analysis of static excitation system models for synchronous machine," *International Journal of Engineering Research & Technology*, vol. 9, no. 9, pp. 64–68, Sep. 2020, doi: 10.17577/IJERTV9IS090027.

[6] S. Nuzzo, M. Galea, C. Gerada, and N. Brown, "Analysis, modeling, and design considerations for the excitation systems of synchronous generators," *IEEE Transactions on Industrial Electronics*, vol. 65, no. 4, pp. 2996–3007, Apr. 2018, doi: 10.1109/TIE.2017.2756592.

[7] J. Machowski, J. W. Bialek, S. Robak, and J. R. Bumby, "Excitation control system for use with synchronous generators," *IEE Proceedings–Generation, Transmission and Distribution*, vol. 145, no. 5, pp. 537–546, Sep. 1998, doi: 10.1049/ip-gtd:19982182.

[8] A. Al-Zahrani and S. K. Ramdas, "Performance evaluation of excitation systems in stability enhancement of power systems," *European Journal of Engineering and Technology Research*, vol. 7, no. 5, pp. 82–93, Oct. 2022, doi: 10.24018/ejeng.2022.7.5.2820.

[9] R. L. Damij, "Development of mechanical coupling and exciter system in synchronous generators," *Eastern-European Journal of Enterprise Technologies*, vol. 6, no. 8 (114), pp. 34–40, 2021, doi: 10.15587/1729-4061.2021.246619.

[10] A. Kutsyk, M. Semeniuk, M. Korkosz, and G. Podskarbi, "Diagnosis of the static excitation systems of synchronous generators with the use of Hardware-In-the-Loop technologies," *Energies*, vol. 14, no. 21, Art. no. 6937, Oct. 2021, doi: 10.3390/en14216937.

[11] R. Wang, X. Liu, and Y. Huang, "Synchronous generator excitation system for a ship based on active disturbance rejection control," *Mathematical Problems in Engineering*, vol. 2021, Art. no. 6638370, Apr. 2021, doi: 10.1155/2021/6638370.

[12] A. Samanfar, M. R. Shakarami, J. Soltani Zamani, and E. Rokrok, "Adaptive sliding mode control for multi-machine power systems under normal and faulted conditions," *Scientia Iranica*, vol. 29, no. 5, pp. 2526–2536, 2022, doi: 10.24200/sci.2020.55717.4371.

[13] A. Alvarez Canabal, V. A. Utkin, A. G. Loukianov, and J. M. Cañedo, "Adaptive controller for a synchronous generator via sliding mode," *IFAC-PapersOnLine*, vol. 55, no. 9, pp. 344–349, 2022, doi: 10.1016/j.ifacol.2022.07.060.

[14] T. K. Roy and M. A. Mahmud, "A nonlinear adaptive excitation controller design for two-axis models of synchronous generators in multimachine power systems to augment the transient stability during severe faults," *IET Generation, Transmission & Distribution*, vol. 16, no. 19, pp. 3906–3927, Oct. 2022, doi: 10.1049/gtd2.12575.

[15] D. C. Karnopp, D. L. Margolis, and R. C. Rosenberg, *System Dynamics: Modeling and Simulation of Mechatronic Systems*, 3rd ed. New York, NY, USA: Wiley-Interscience, 2000.

[16] J. Thoma and B. Ould Bouamama, *Modelling and Simulation in Thermal and Chemical Engineering*. Berlin, Germany: Springer-Verlag, 2000, doi: 10.1007/978-3-662-04181-9.

[17] H. Wang and D. A. Linkens, *Intelligent Supervisory Control: A Qualitative Bond Graph Reasoning Approach*. Singapore: World Scientific, 1996, doi: 10.1142/3098.

[18] C. Sueur and G. Dauphin-Tanguy, "Bond-graph approach for structural analysis of MIMO linear systems," *Journal of the Franklin Institute*, vol. 328, no. 1, pp. 55–70, 1991, doi: 10.1016/0016-0032(91)90006-O.

[19] G. Gonzalez Avalos and N. Barrera Gallegos, "Quasi-steady state model determination for systems with singular perturbations modelled by bond graphs," *Mathematical and Computer Modelling of Dynamical Systems*, vol. 19, no. 5, pp. 483–503, 2013, doi: 10.1080/13873954.2013.766214.

[20] A. Merabtine, "An integrated bond graph methodology for building performance simulation," *Energies*, vol. 18, no. 15, Art. no. 4168, Aug. 2025, doi: 10.3390/en18154168.

[21] G. Srinivasarao, A. K. Samantaray, and S. K. Ghoshal, "Bond graph modeling and multi-body dynamics of a twin rotor system," *Proceedings of the Institution of Mechanical Engineers, Part I: Journal of Systems and Control Engineering*, vol. 235, no. 1, pp. 117–144, 2021, doi: 10.1177/0959651819899267.

[22] P. J. Gawthrop, M. Pan, and E. J. Crampin, "Modular dynamic biomolecular modelling with bond graphs: The unification of stoichiometry, thermodynamics, kinetics and data," *Journal of The Royal Society Interface*, vol. 18, no. 181, Art. no. 20210478, Aug. 2021, doi: 10.1098/rsif.2021.0478.

[23] W. Ai, P. J. Hunter, M. Pan, and D. P. Nickerson, "Energetic analysis of Na^+/K^+-ATPase using bond graphs," *bioRxiv*, preprint, May 2026, doi: 10.64898/2026.04.05.716446.

[24] P. Gawthrop and M. Pan, "Energy-based analysis of biochemical oscillators using bond graphs and linear control theory," *Royal Society Open Science*, vol. 12, no. 4, Art. no. 241791, Apr. 2025, doi: 10.1098/rsos.241791.

[25] J. Forrest, V. Rajagopal, M. P. H. Stumpf, and M. Pan, "BondGraphs.jl: Composable energy-based modelling in systems biology," *Bioinformatics*, vol. 39, no. 10, Art. no. btad578, Oct. 2023, doi: 10.1093/bioinformatics/btad578.

[26] X. Zhou and Y. Cui, "Dynamic characteristics of single-loop gear system based on bond graph method," *Journal of Vibroengineering*, vol. 24, no. 3, pp. 604–614, May 2022, doi: 10.21595/jve.2021.22290.

[27] J. Wu, H. Yan, S. Liu, Y. Zhang, and W. Tan, "Bond graph-based approach to modeling variable-speed gearboxes with multi-type clutches," *Applied Sciences*, vol. 12, no. 12, Art. no. 6181, Jun. 2022, doi: 10.3390/app12126181.

[28] D. Sahm, "A two-axis, bond graph model of the dynamics of synchronous electrical machines," *Journal of the Franklin Institute*, vol. 308, no. 3, pp. 205–218, Sep. 1979, doi: 10.1016/0016-0032(79)90113-3.

[29] A. Ramdane, A. Lachouri, and M. Krikeb, "Modeling and simulation of a wind turbine driven induction generator using bond graph," *Journal of Renewable Energy and Sustainable Development*, vol. 1, no. 2, pp. 236–242, Dec. 2015, doi: 10.21622/resd.2015.01.2.236.

[30] T. Bakka and H. R. Karimi, "Bond graph modeling and simulation of wind turbine systems," *Journal of Mechanical Science and Technology*, vol. 27, no. 6, pp. 1843–1852, Jun. 2013, doi: 10.1007/s12206-013-0435-x.

[31] B. Umesh Rai and L. Umanand, "Bond graph model of doubly fed three phase induction motor using the Axis Rotator element for frame transformation," *Simulation Modelling Practice and Theory*, vol. 16, no. 10, pp. 1704–1712, Nov. 2008, doi: 10.1016/j.simpat.2008.08.012.

[32] G. Gonzalez-Avalos, G. Ayala-Jaimes, N. Barrera-Gallegos, and A. Padilla Garcia, "Modeling and simulation of an integrated synchronous generator connected to an infinite bus through a transmission line in bond graph," *Symmetry*, vol. 16, no. 10, Art. no. 1335, 2024, doi: 10.3390/sym16101335.

[33] G. Gonzalez-Avalos, G. Ayala-Jaimes, T. Lopez-L, and A. A. Castillo Barron, "Modeling and simulation of balanced systems formed by synchronous generator-infinite bus in a multi-bond graph approach," *WSEAS Transactions on Systems and Control*, vol. 19, pp. 407–414, 2024, doi: 10.37394/23203.2024.19.44.

Contribution of Individual Authors to the Creation of a Scientific Article (Ghostwriting Policy) The authors equally contributed in the present research at all stages, from the formulation of the problem to the final findings and solution.

Sources of Funding for Research Presented in a Scientific Article or Scientific Article Itself
No funding was received for conducting this study.

Conflicts of Interest
The authors have no conflicts of interest to declare.

Creative Commons Attribution License 4.0 (Attribution 4.0 International , CC BY 4.0)
This article is published under the terms of the Creative Commons Attribution License 4.0
https://creativecommons.org/licenses/by/4.0/deed.en_US